

Evaluation of the Biological Impact of Chronic Exposure to Aerosol From Flavored E-Liquids on Respiratory Organs of the A/J Mouse

K. Luettich[#], E. Wong^{*}, M.A. Choukrallah[#], Y. Xiang[#], A. Sewer[#], A.R. Kolli[#], L. Khachatryan[#], E. Guedj[#], J. Zhang[@], B. Langston[@], K. M. Lee^{@‡}, D. Sciuscio[#], P. Vanscheeuwijck[#].

^{*} PMI R&D, Philip Morris International Research Laboratories Pte Ltd, Singapore; [#] PMI R&D, Philip Morris Products S.A., Neuchâtel, Switzerland; [@] Altria Client Services LLC, Richmond, VA, U.S.A.; [‡] Former employee



Introduction and Objectives

To assess the impact of lifetime exposure to flavored e-vapor aerosol compared with 3R4F cigarette smoke (CS), A/J mice were exposed to flavored e-vapors with and without nicotine (N). Histopathological evaluation of respiratory tract organs and non-respiratory tissues was performed following chronic exposure, with key results presented elsewhere (Poster 4910/P770). In this study, we evaluated nasal epithelium, larynx, and lungs using transcriptomics and genomics analyses to gain insights into the potential biological impact of exposure effects in this mouse strain.

Study Design

A/J mice (Jackson Laboratory, Bar Harbor, ME, USA) were whole-body exposed to filtered air (Sham), aerosol from carriers propylene glycol (PG) and vegetable glycerol (VG), PG/VG with nicotine (PG/VG/N, 2% [w/w]), PG/VG/N with flavors (F) at low, medium, and high concentrations (PG/VG/N/F - 1.2 to 18.6% [w/w]), PG/VG/F-H or to mainstream CS from the 3R4F reference cigarette for 6 h/day, 5 days/week for up to 18 months. The target nicotine aerosol concentration was 15 µg/L. The study design (Figure 1) generally followed the OECD Test Guideline 453. The care and use of mice were in accordance with the National Advisory Committee for Laboratory Animal Research Guidelines and approved by the Institutional Animal Care and Use Committee.

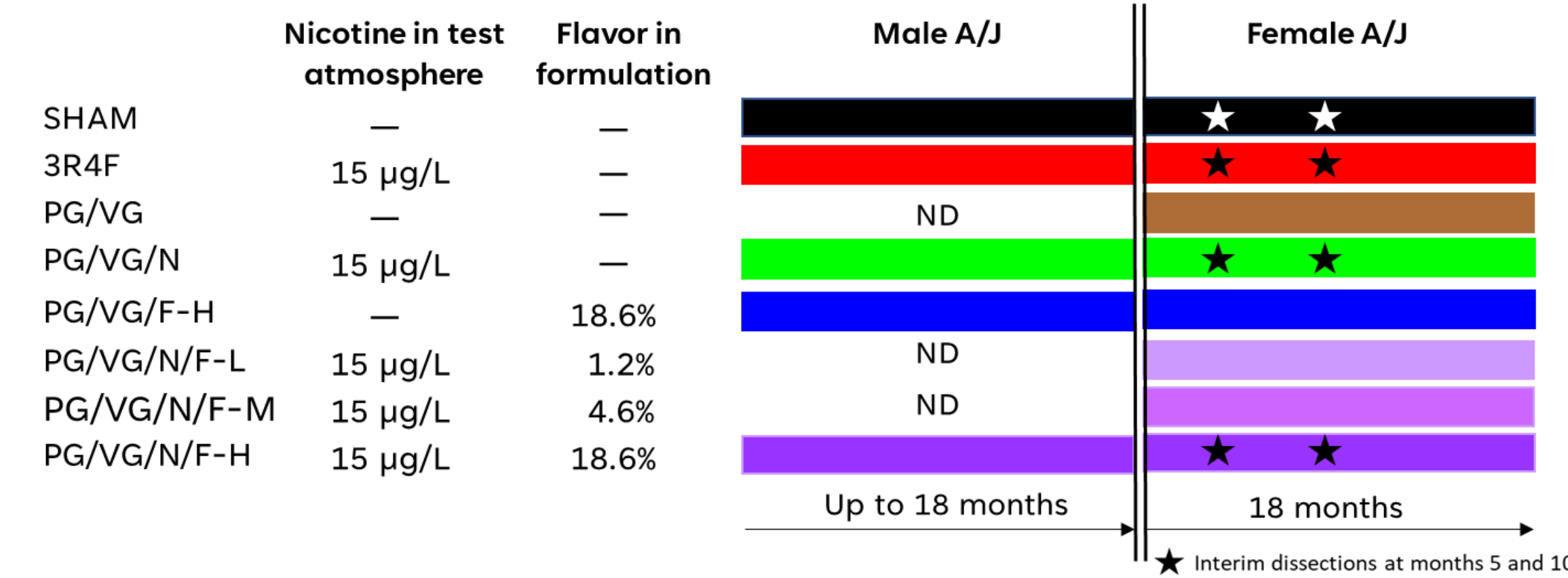


Figure 1. Schematic overview of study design.

To maintain a minimum number of mice for terminal dissection, the male mice were dissected beginning month 17, while female mice were dissected beginning month 18 of the study. PG: propylene glycol; VG, vegetable glycerol; N, nicotine; F-X, flavor(-concentration); L, low; M, medium; H, high; ND, not done.

At the interim and terminal dissection time points, nasal epithelial, laryngeal, and lung* tissues were collected for transcriptomics analysis using Affymetrix microarrays, untargeted proteomics analysis using an iTRAQ[®]-based quantitative approach, and whole genome sequencing analyses. Data presented here are from the terminal dissection time point, except for the tumor classification results (inclusive of all time points).

* Note: Laser-capture microdissection (LCM) was used to specifically collect lung parenchymal or tumor tissue from each left lung under the guidance of the Study Pathologist.

Results

1. E-vapor aerosol exposure has minimal biological impact on the lungs

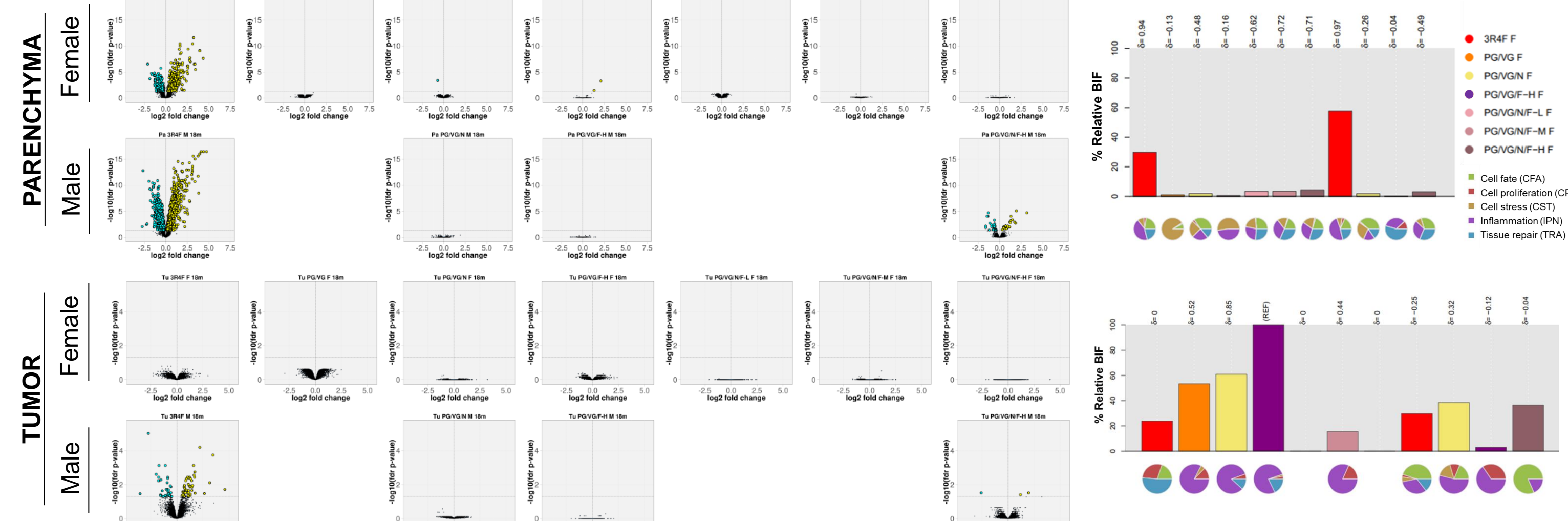


Figure 2: Gene expression profile in lung parenchyma (upper panel) and lung tumors (lower panel). The gene expression changes for each gene, calculated as the log₂ fold change, are plotted on the x-axis and the statistical significance, proportional to the -log₁₀ of the FDR p-value, is plotted on the y-axis. Yellow and cyan dots indicate genes that were statistically significantly up- or down-regulated, respectively (right and left quadrants, respectively) compared to the Sham group. The comparison group is indicated on top of each plot. N = 9–15. PG, propylene glycol; VG, vegetable glycerol; N, nicotine; F(-X), flavor(-concentration); L, low; M, medium; H, high; FDR, false discovery rate.

Figure 3: Network model-based analysis of the biological impact factor (BIF) on lung parenchyma (top) and lung tumors (bottom). The bar plot depicts BIF values relative to the maximum response or reference (RBIF = 100%, REF). The δ values (-1 to 1) indicate how similar the underlying network perturbations are with respect to the REF.

2. Tumor classification using a 13-gene signature indicates no significant differences between tumors from mice exposed to e-vapor aerosol and Sham

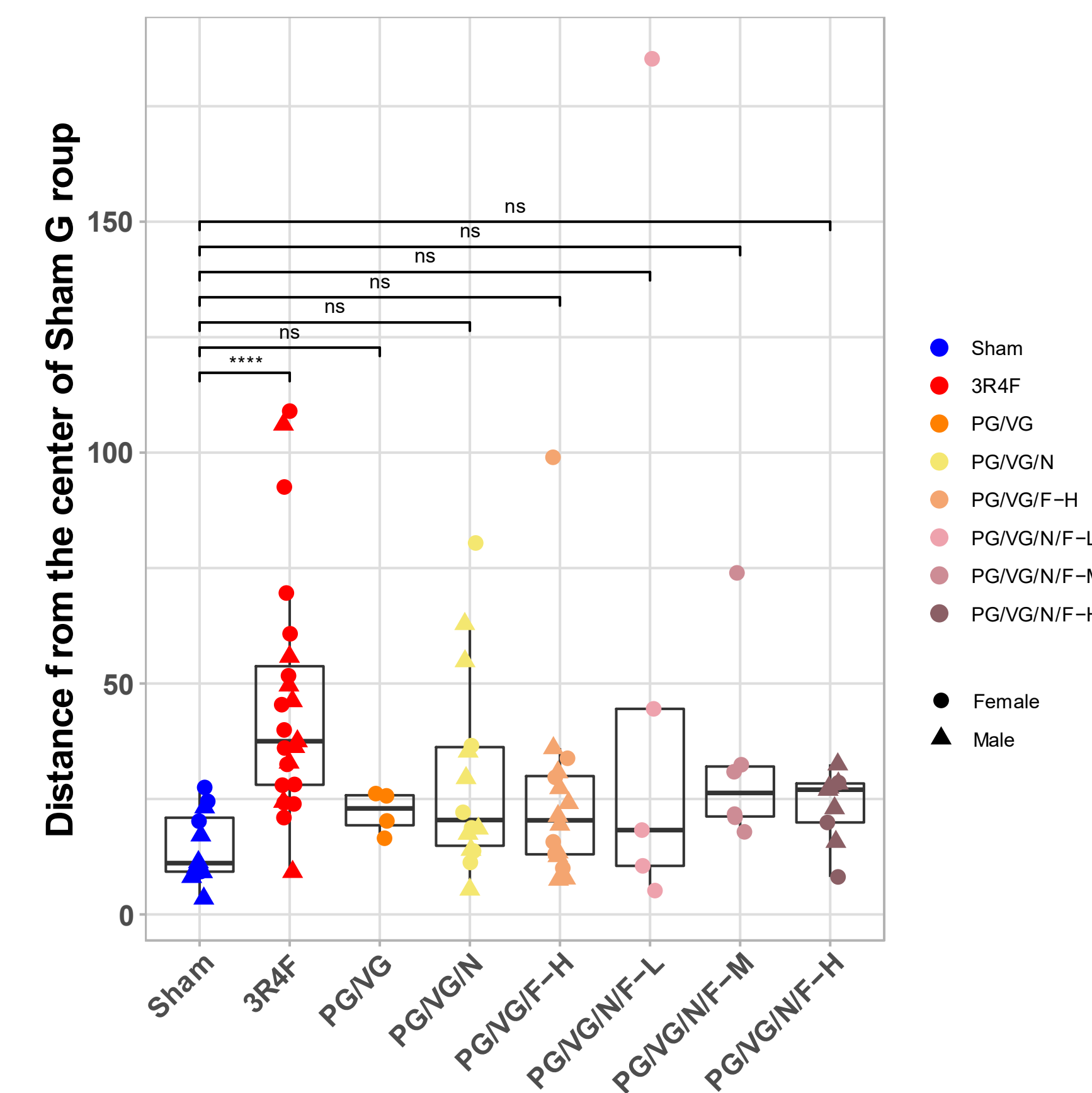


Figure 4. Estimates of similarity between lung tumors based on Mahalanobis distance. As an estimate of similarity between lung tumors, the Mahalanobis distance between lung tumors in Sham animals and those in each test condition was calculated based on a 13-gene signature derived from an interaction analysis of gene expression data from a previous A/J study (E-MTAB-1871). Results are presented as mean ± standard error of the mean (SEM). N = 6–16. *** p < 0.001; ns: not significant. PG, propylene glycol; VG, vegetable glycerol; N, nicotine; F(-X), flavor(-concentration); L, low; M, medium; H, high.

3. Genetic profiles of lung tumors from e-vapor-exposed mice are distinct from those of CS-exposed mice

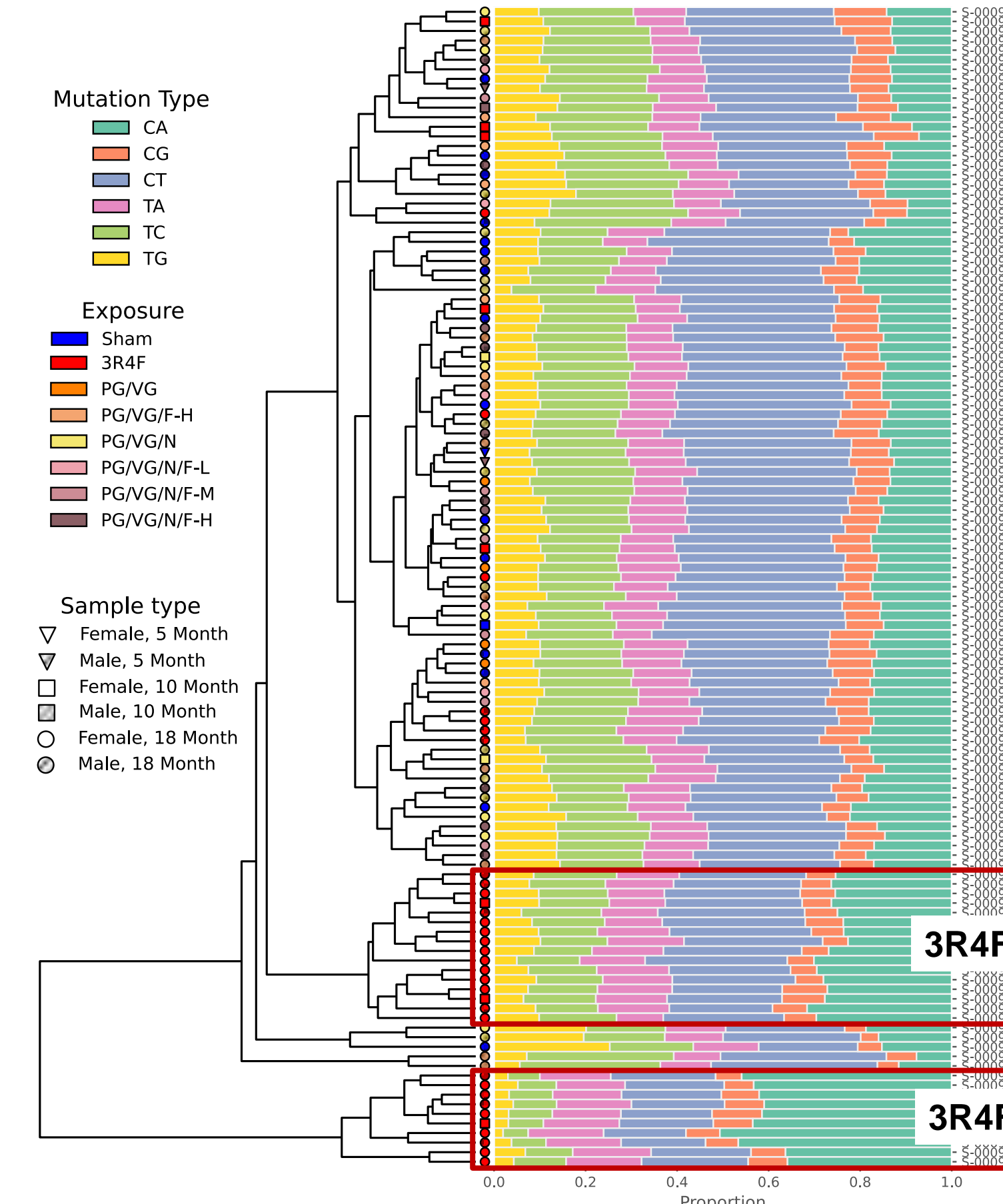


Figure 5. Relative proportion of the six mutation types in lung tumors. Proportions of each of the six mutation types (C→A, C→G, C→T, T→A, T→C, T→G, indicated by different colors, see legend) for each tumor sample are shown as stacked bar chart. Tumor samples are indicated by their study group designation (designated by colored symbols) and sample ID listed on the right side. The dendrogram on the left reflects the clustering of the samples based on the relative proportion of each base substitution type displayed in the bar chart.

Results

4. DNA methylation patterns are less affected by e-vapor exposure than by CS exposure

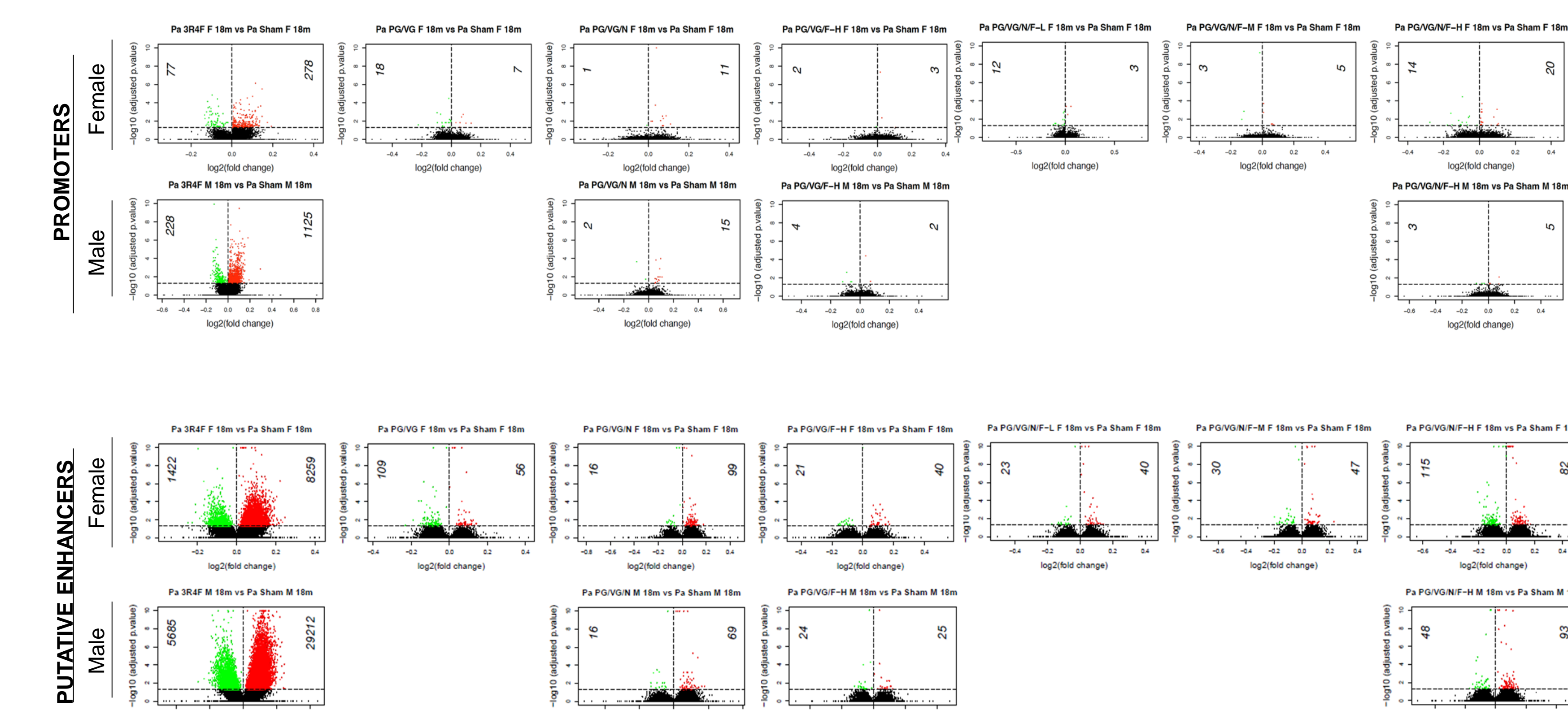


Figure 6. Lung parenchyma DNA methylation profiles at promoter (upper panel) or putative enhancer loci (lower panel). Volcano plots representing the amplitude and significance of methylation changes at promoters and putative enhancer loci in lung parenchyma between the indicated exposure group and the Sham group. Methylation difference (exposure - control) is plotted on the x-axis and the statistical significance, proportional to the -log₁₀ of the FDR p-value, is plotted on the y-axis. Red and green dots indicate hyper- and hypomethylated loci, respectively, relative to the Sham group. The comparison for each exposure group is indicated on top of each plot. N = 6–16. PG, propylene glycol; VG, vegetable glycerol; N, nicotine; F(-X), flavor(-concentration); L, low; M, medium; H, high; FDR, false discovery rate.

4. High flavor concentrations in e-vapor have a bigger impact on nasal than on laryngeal epithelium

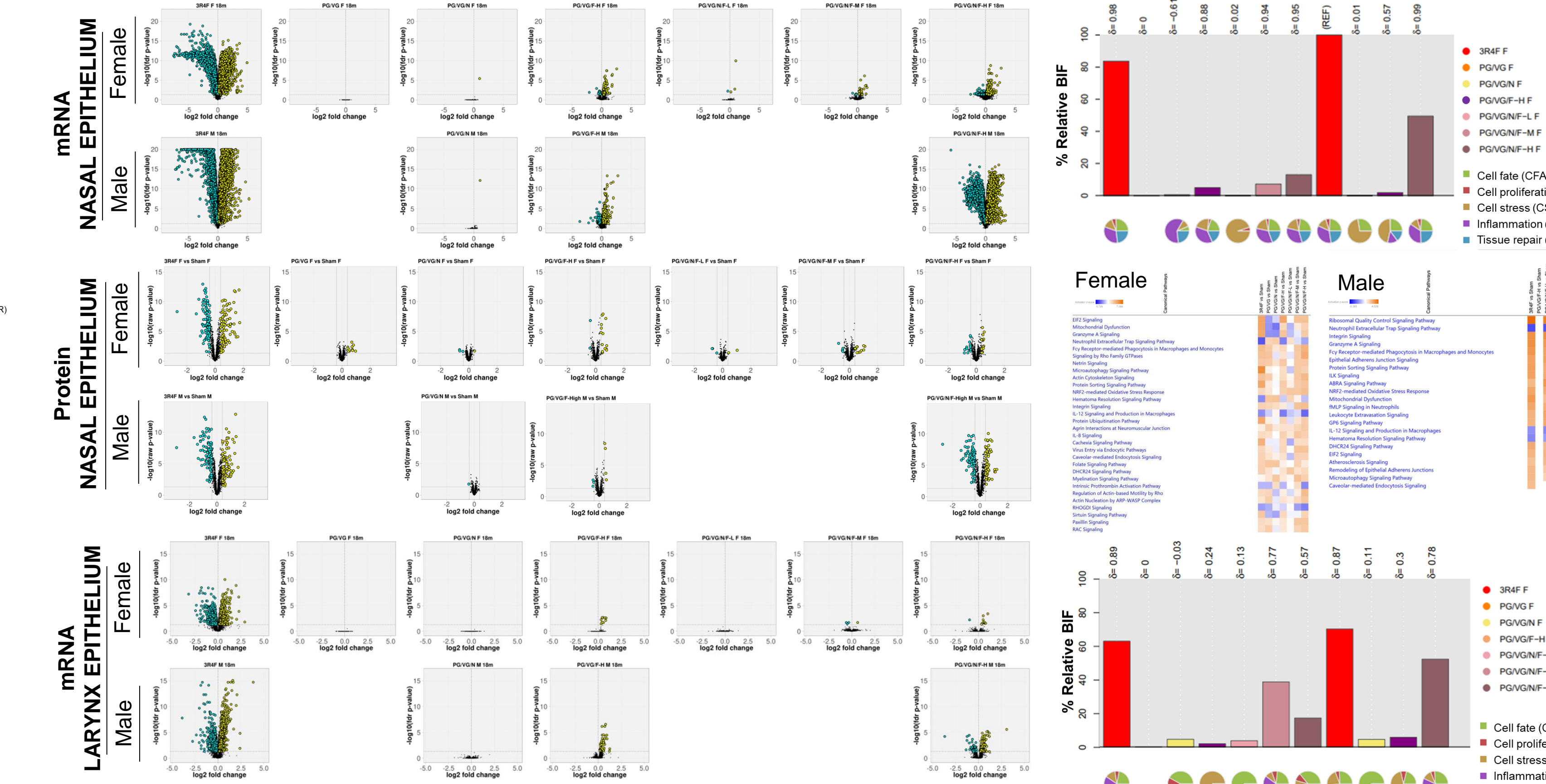


Figure 7: Gene (top panel) and protein (middle panel) expression profiles in nasal epithelium, and gene expression profile in larynx (bottom panel).

Figure 8: Network model-based analysis of the biological impact factor (BIF) on nasal epithelium.

Figure 9: Enrichment analysis of differentially abundant proteins in the laryngeal epithelium, with a focus on canonical signaling pathways (Ingenuity Pathway Analysis[®]). Results were filtered by z-score > |2| and p-value < 0.05. For females, only the top 30 pathways are shown.

Figure 10: Network model-based analysis of the biological impact factor (BIF) on laryngeal epithelium.

Summary and Conclusions

The biological effects of chronic e-vapor aerosol exposure were less pronounced than those of cigarette smoke exposure. Chronic cigarette smoke exposure caused extensive changes in the nasal epithelial transcriptome, impacting various mechanisms including stress responses, inflammation, and tissue remodeling. Untargeted proteomics corroborated these results with similar biological processes being affected by all exposures, with a notably smaller impact of e-vapor aerosol than cigarette smoke exposure on proteins related to stress, immune, and inflammatory responses. Together these alterations may underpin the histopathological observations in the olfactory epithelium that are potentially related to irritation from repeated exposure.

Lung parenchyma mRNA profiles from e-vapor groups exhibited minimal to no significant changes, which corresponds to minimal or absent histological changes. In contrast, in lung parenchyma, cigarette smoke exposure resulted in marked changes in genes involved in inflammation, immune responses, and cell proliferation, among others. Lung tumor gene expression was less affected by exposure to either cigarette smoke or e-vapor aerosol than lung parenchyma, with no significant changes detected in female mice.

Gene signature analysis for tumor classification revealed a notable difference between lung tumors from e-vapor aerosol-exposed and Sham mice compared to those from cigarette smoke-exposed mice. DNA analysis highlighted differences in the mutational spectra as well as in the DNA methylation profile of tumors from Sham, e-vapor aerosol-, and CS-exposed mice.

The biological effects of chronic e-vapor aerosol exposure appear to be driven by high flavor concentrations, independent of nicotine. Exposure to high flavor concentrations also impacted gene expression in the laryngeal epithelium, though to a lesser degree than in the nasal epithelium, and markedly less than cigarette smoke exposure. Cell fate mechanisms were affected together with inflammatory and tissue remodeling processes in cigarette smoke-exposed mice, aligning with the observed advanced adaptive epithelial changes in the larynx. The miRNAome was minimally altered, independent of the test atmosphere.

Together, these findings present a unique view of the molecular processes in respiratory tract tissues following chronic exposure to flavored e-vapor aerosol or cigarette smoke. It demonstrates the reduced risk potential of e-vapor products compared to combustible cigarette smoke and the potential role of e-vapor products in tobacco harm reduction.